Erzinger, J., Becker, K., Dick, H.J.B., and Stokking, L.B. (Eds.), 1995
Proceedings of the Ocean Drilling Program, Scientific Results, Vol. 137/140

22. ROCK MAGNETISM AND MAGNETIC MINERALOGY OF A 1-KM SECTION OF SHEETED DIKES, HOLE 504B[1]

Janet E. Pariso,[2] Laura Stokking,[3] and Simon Allerton[4]

ABSTRACT

Magnetic properties and oxide petrography results are presented from dike samples recovered during Ocean Drilling Program Legs 137 and 140 at Hole 504B on the Costa Rica Rift. Although secondary magnetite is common, the most abundant magnetic phase is low-titanium magnetite produced during oxidation of primary (igneous) titanomagnetite. In general, titanomagnetite grains in the Leg 137/140 dike samples were observed to have experienced substantially higher degrees of high-temperature deuteric oxidation than the upper portion of the dike complex, suggesting a gradual decrease in the rate of cooling with depth. Paleomagnetic measurements indicate that samples recovered during Legs 137 and 140 acquired a component of drilling-induced remanent magnetization. However, stable magnetic inclinations determined after alternating-field demagnetization indicate the direction of the hardest component of magnetization is very near that predicted for this equatorial site (0°). The average intensity of natural remanent magnetization for the entire dike complex is 2.1 A/m, about half that observed for the overlying extrusive basalts. Room temperature rock magnetic measurements indicate that the effective magnetic grain size of the dike samples falls within the region described as pseudo-single domain. Together, these results suggest that the sheeted dike complex sampled at Hole 504B is capable of contributing to the anomaly observed at sea surface.

INTRODUCTION

The recent success of Ocean Drilling Program (ODP) Legs 137 and 140 at Hole 504B on the Costa Rica Rift resulted in a penetration of 438 m and a final Leg 140 depth of 2000.5 meters below seafloor (mbsf) making Hole 504B the deepest hole in oceanic crust and the only drill hole to penetrate through the extrusive basalts and sheeted dike complex. Hole 504B is our most complete reference section of in-situ oceanic crust and thus provides a singular opportunity to study the geophysical and geological properties of oceanic Layer 2C and to develop a better understanding of the processes that control the formation and evolution of upper oceanic crust. In this paper, we examine the magnetic properties and magnetic mineralogy of diabase dike samples recovered from Hole 504B. We combine results from our Leg 137/140 samples with data previously published by Smith and Banerjee (1986) and Pariso and Johnson (1989; 1991). Our goal is to describe the vertical magnetic structure of the dike complex, characterize the post-emplacement processes that affect the magnetic minerals in the dike rocks, and evaluate the ability of these intrusive crustal rocks to contribute to marine magnetic anomalies.

GEOLOGICAL SETTING

Hole 504B is located on the south flank of the Costa Rica Rift (Fig.1) in crust that is approximately 5.9 Ma. Regional studies show that heat flow values at Site 504 approach those expected for a conductively cooling lithospheric plate (Anderson and Hobart, 1976; Langseth et al., 1983). Thus, although there is substantial lithologic evidence that a hydrothermal system was once active within the 504B crustal section (Honnorez et al., 1983; Alt et al., 1986), it appears that no significant crustal cooling is currently taking place by such a mechanism. Consistent with this, the equilibrium temperature at the bottom of the hole was estimated to be 200°C based on downhole measurements performed during Leg 137 (Becker, Foss, et al., 1992; Gable et al., this volume).

Drilling at Hole 504B has involved six separate DSDP/ODP legs through Leg 140 and has shown that the crustal section is composed of three distinct lithologic zones: a 570-m section of extrusive basalts, a 200-m transition zone consisting of both dikes and extrusive basalts, and a 945-m section of basaltic dikes (see Becker et al., 1989, for a review; also Fig. 2). Based on secondary mineralogy, three distinct alteration zones have been identified and include an upper zone of low-temperature oxidative alteration, a middle zone of low-temperature suboxic to anoxic alteration, and a lower zone characterized by greenschist facies minerals and lower amphibolite facies minerals (Alt et al., 1989; Alt, Zuleger, and Erzinger, this volume). The dike section lies entirely within the lower, greenschist/amphibolite facies alteration zone.

METHODS

Measurements of natural remanent magnetization (NRM) were made on minicores aboard the *JOIDES Resolution* using a 2-G cryogenic magnetometer and at the University of Washington using a Schonstedt spinner magnetometer. Stepwise alternating field demagnetization (AFD) was performed using a Schontstedt model GS-1 demagnetizer. Individual components of remanent magnetization were identified using orthogonal vector diagrams (Zijderveld, 1967), and the directions of the individual components were calculated using a least-squares fitting routine. Magnetic susceptibility was measured using a Bartington Model MS-1 susceptibility meter. Rock magnetic measurements were performed at the Institute of Rock Magnetism at the University of Minnesota and at Scripps Institute of Oceanography. Hysteresis loop parameters were measured on large (e.g., 1 g) chips using a Princeton Applied Research vibrating sample magnetometer (VSM) and on smaller chips (e.g., 0.03 to 0.05 g) using a Princeton Applied Research alternating gradient force magnetometer. Although different sample sizes were required for the two magnetometers, the agreement between chips from the same minicore was usually very good. This was expected because of the relatively fine grain size of the diabase dikes being studied. Curie temperature measurements were performed using an oven on the Princeton Applied Research VSM.

Paleomagnetic and rock magnetic data for Leg 137/140 samples are displayed in Tables 1 and 2, respectively. Mean values of paleomagnetic and rock magnetic parameters for Leg 137/140 samples are

[1] Erzinger, J., Becker, K., Dick, H.J.B., and Stokking, L.B. (Eds.), 1995. *Proc. ODP, Sci. Results*, 137/140: College Station, TX (Ocean Drilling Program).
[2] School of Oceanography, University of Washington, Seattle, WA 98195, U.S.A.
[3] Ocean Drilling Program, Texas A&M University Research Park, College Station, TX 77845-9547, U.S.A.
[4] Department of Earth Sciences, University of Oxford, Parks Road, Oxford OX1 3PR, United Kingdom.

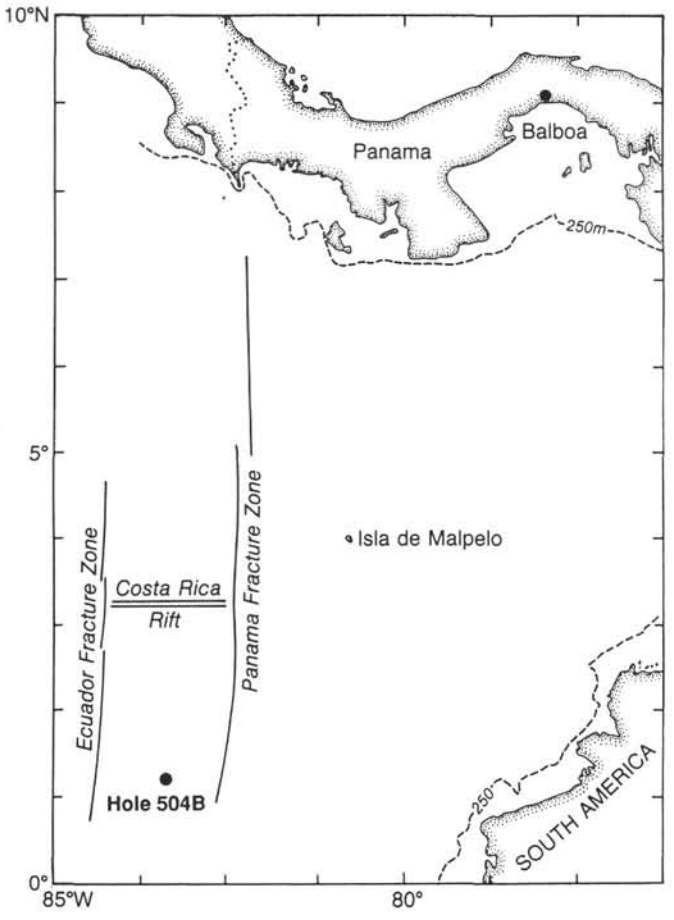

Figure 1. Location of Hole 504B on the south flank of the Costa Rica Rift in the equatorial Pacific Ocean.

summarized in Table 3. Mean values of paleomagnetic and rock magnetic parameters for the entire dike complex samples at Hole 504B are displayed in Table 4.

RESULTS

Natural Remanent Magnetization

Values of the intensity of natural remanent magnetization (J_0) are plotted vs. depth for the entire sheeted dike complex in Figure 3. J_0 values increase with depth, and the mean J_0 value of the entire dike section is 2.1 A/m. This value is about half of the J_0 value observed for the extrusive basalts at Hole 504B (5.6 A/m). Although most of the J_0 values are greater than 1 A/m, a significant number of samples have values much lower than this (<0.1 A/m). Magnetic susceptibility (k) values are plotted vs. depth in Figure 3. Similar to J_0 values, k values increase slightly with depth (note these parameters are plotted on a log scale). The mean k value for the entire dike complex is 0.017 SI, and this is very close to the value observed for the overlying extrusive basalts (0.019 SI). In parallel with J_0 values, most k values are moderately high (>0.01), but a significant number of samples have dramatically lower k values (<0.001). Examination of the minicores shows that the samples with very low J_0 and k values have experienced very high degrees of hydrothermal alteration, whereas samples with moderate to high J_0 and k values have experienced much smaller degrees of alteration. This is consistent with the petrologic observation that most of the recovered core was observed to have 10%–20% secondary minerals, and about 10% of the core samples have 60%–80% secondary minerals (Alt, Zuleger, and Erzinger, this volume).

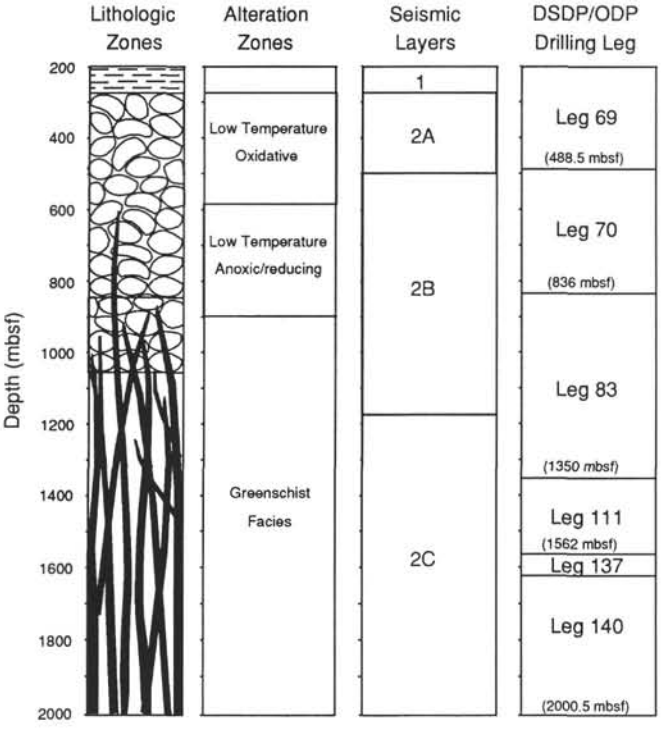

Figure 2. Summary of lithologic zones, alteration zones (Alt et al., 1986), seismic layers (Newmark et al., 1985), and drilling history at Hole 504B.

The Koenigsberger, or Q, ratio compares the magnitude of the remanent magnetization to the instantaneous magnetization induced in the sample by the Earth's field. Q values were calculated for Hole 504B samples using the equation $Q = J_0/(k \cdot H)$, where H is the value of the geomagnetic field at Site 504 (0.033 mT). Q values are plotted in Figure 3. This plot shows that nearly all of the samples have values greater than 1 and are thus dominated by remanent, rather than induced, magnetization. Because it is the remanent magnetization that records reversals of the Earth's magnetic field, this becomes a particularly important fact to establish when assessing the ability of this crustal section to contribute to marine magnetic anomalies.

The value of the demagnetizing field required to remove half of the NRM is referred to as the median demagnetizing field (MDF). MDF values for the Hole 504B dike samples are plotted in Figure 3 and show a significant decrease as a function of depth. The mean MDF value for the entire dike complex is 17.2 mT and indicates that most of the dikes are relatively resistant to AF demagnetization. This implies that the remanent magnetization is stable. However, the lower dikes, and particularly the Leg 137/140 samples, have very low MDF values, and this indicates their NRM is less stable. Rock magnetic parameters, which will be discussed in the next section, indicate that the effective magnetic grain size of the 504B dikes increases with depth. Large magnetic grain sizes result in remanent magnetization that is unstable or easily changed (e.g., Day et al., 1977). As we will discuss later, the increase in effective magnetic grain size correlates with a gradual change in the style of alteration of magnetite. Thus the change in alteration of magnetite with depth is likely responsible for the decrease in MDF values. The mean MDF value of the 504B sheeted dikes is higher than that of the overlying extrusives (7.2 mT), indicating that, overall, the dikes have a more stable remanent magnetization. However, the lower dikes exhibit MDF values that are comparable to the extrusive basalts.

Values of the inclination of NRM (I_{nrm}) and the inclination of stable remanent magnetization (I_{stable}) are plotted in Figure 4. Based on a geocentric axial dipole field, the magnetic inclination predicted for Site 504 is approximately zero. The mean I_{stable} value for all of the

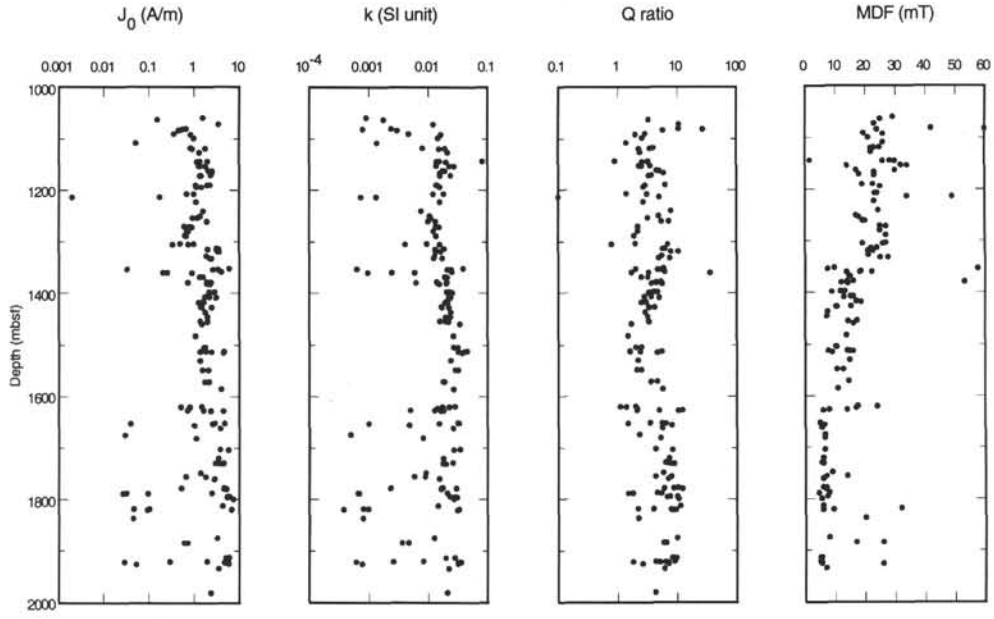

Figure 3. Intensity of NRM (J_0), magnetic susceptibility (k), Q ratio, and mean demagnetization field (MDF) plotted vs. depth for 504B dike samples. Note that J_0, k, and Q are plotted on log scales.

504B dike samples is –5° and is thus very close to the value expected for this latitude. Comparison of Figure 4 shows that samples recovered above 1560 m have similar I_{nrm} and I_{stable} values. This indicates that although small components of secondary magnetization were sometimes observed, these samples have only one significant component of remanent magnetization. In contrast, samples recovered below 1560 mbsf are observed to have distinctly different I_{nrm} and I_{stable} values. The secondary components of magnetization for these samples were always very steep and negative (i.e., –80° or more). Because the secondary magnetization has a steep inclination, it seems unlikely that it was acquired parallel to the Earth's magnetic field (which is close to horizontal at this latitude) during a natural geological process. In addition, the secondary components of magnetization were completely removed at very low demagnetization levels (e.g., by 7.5 mT). Together, these observations suggest that the secondary magnetization observed in samples recovered below 1560 m is a drilling-induced remanent magnetization (DIRM). DIRM has been previously observed in core samples recovered during DSDP/ODP legs (Ade-Hall and Johnson, 1976; Lowrie and Kent, 1978; Pariso et al., 1991). DIRM is typically steeply inclined and very soft magnetically. It has been suggested to be a piezo-remanent magnetization resulting from the shock of rotary core drilling, or a viscous or isothermal remanent magnetization acquired as the drill core is pulled to the ship through the drill string.

For the 504B dike samples, components of DIRM are only present in samples recovered during Legs 137 and 140. There are two possible causes for the sudden appearance of DIRM at 1560 mbsf. First, rock magnetic properties (discussed fully in the next section) indicate that the effective magnetic grain size of the 504B dikes increases with depth. This indicates that the remanent magnetization of the dike complex is becoming increasingly unstable. Therefore the potential to acquire secondary forms of magnetization is high. However, the DIRM appears very suddenly at 1560 m, whereas the magnetic grain size increase is observed to occur gradually with depth. It is possible that the effective magnetic grain size reaches a threshold value, and that beyond this value, DIRM is easy to acquire. Another possibility is that the DIRM components are related to an abrupt change in the drilling system itself. For example, a very magnetic bottom hole assembly (BHA) could result in the appearance of DIRM in the dike samples. Examination of the operations records from Legs 111, 137, and 140 indicates that the only significant change in the BHA during these different legs is an increase in the number of drill collars that make up the BHA (Becker et al., 1989; Becker, Foss, et al., 1992; Dick, Erzinger, Stokking, et al., 1992). Because there is a weak magnetic field associated with the drill collars, a larger number of drill collars could result in a field sufficient to induce an isothermal remanent magnetization in the recovered samples. Unfortunately, this is a somewhat difficult theory to test, as it requires measuring the magnetic field associated with different numbers of drill collars. We suggest that the factors responsible for acquisition of DIRM are complex and that the gradual increase in effective magnetic grain size with depth plays an important role in the acquisition of DIRM.

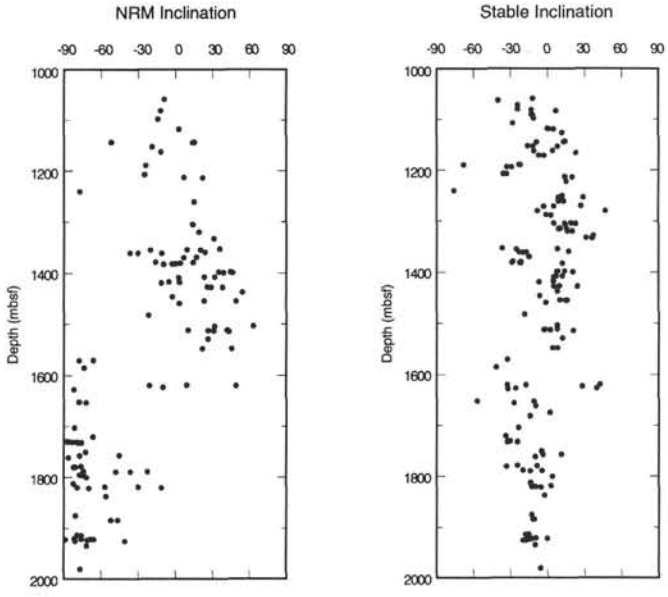

Figure 4. Inclination of natural remanent magnetization (I_{nrm}) and stable remanent magnetization (I_{stable}) plotted vs. depth for 504B dike samples.

Figure 4 shows a small but discernable change in I_{stable} values at approximately 1560 mbsf. The somewhat steeper I_{stable} values below

Table 1. Summary of paleomagnetic measurements for Leg 137/140 dike samples.

Core, section, interval (cm)	Depth	NRM (A/m)	k (SI units)	Q	MDF (mT)	I_{anc}	I_{stable}
137-504B-							
173R-2, 20–22	1571.70	1.74E+00	1.86E–02	3.6	ND	–77.5	ND
175R-1, 19–21	1585.99	4.03E+00	2.68E–02	5.7	11	–73.6	–41.6
180M-1, 92–94	1619.32	1.49E+00	2.81E–02	2.0	17.5	9.4	42.5
180M-2, 29–31	1620.19	5.20E–01	1.74E–02	1.1	24	–20.8	–32.4
180M-2, 49–51	1620.39	8.10E–01	2.25E–02	1.4	ND	49.4	–17.5
181M-2, 148–150	1623.38	7.81E–01	1.42E–02	2.1	17	–9.6	28.1
140-504B-							
186R-1, 54–56	1626.84	1.63E+00	5.00E–03	12.4	8	ND	39.7
186R-1, 81–83	1627.11	7.21E–01	1.28E–02	2.1	14	ND	–25.5
186R-1, 121–123	1627.51	2.38E+00	1.82E–02	5.0	ND	–81.7	ND
186R-2, 42–44	1628.22	4.52E+00	1.64E–02	10.5	6	ND	–32.1
189R-1, 96–98	1651.96	2.90E+00	3.14E–02	3.5	5	ND	–57.2
189R-1, 101–103	1652.01	4.86E+00	3.29E–02	5.6	ND	–77.7	ND
189R-2, 39–41	1652.89	2.60E+00	1.52E–02	6.5	5	ND	–11.2
189R-2, 72–74	1653.22	4.00E–02	1.01E–03	1.5	ND	–72.2	ND
190R-1, 95–97	1656.05	1.03E+00	4.80E–03	8.2	6.5	ND	–27.3
191R-1, 48–50	1661.88	3.83E+00	2.62E–02	5.6	5.5	ND	–9.7
193R-1, 48–50	1674.98	3.00E–02	4.90E–04	2.3	6.5	ND	1.9
194R-1, 92–94	1681.32	1.11E+00	8.11E–03	5.2	6.5	ND	–14.2
197R-1, 32–34	1703.12	3.78E+00	3.38E–02	4.3	ND	–81.2	ND
197R-1, 131–133	1704.11	5.82E+00	2.68E–02	8.3	6.5	ND	–23.5
199R-1, 121–123	1720.61	3.47E+00	1.80E–02	7.3	6	–66.6	–33.8
200R-1, 109–111	1729.69	2.97E+00	1.80E–02	6.3	ND	–87.6	ND
200R-1, 128–130	1729.88	4.53E+00	2.57E–02	6.7	5.5	–85.7	–30.1
200R-2, 44–46	1730.54	3.47E+00	1.82E–02	7.2	6	–79.4	–31.7
200R-2, 73–75	1730.83	3.55E+00	1.75E–02	7.7	ND	–83.1	ND
200R-2, 140–142	1731.50	4.43E+00	1.98E–02	8.5	6	–75.6	–24.5
200R-3, 13–15	1731.73	4.39E+00	1.88E–02	8.9	6	–78.4	–32.7
203R-1, 57–59	1749.57	1.39E+00	9.10E–03	5.8	9	–72.3	–4.8
204R-1, 8–10	1756.58	6.60E–01	5.78E–03	4.3	14	–45.2	11.2
205R-1, 3–5	1757.03	1.82E+00	8.81E–03	7.9	7	–76.9	–3.7
206R-1, 19–21	1760.89	2.81E+00	1.52E–02	7.0	6	–86.2	–9.9
208R-1, 4–6	1778.04	4.66E+00	1.74E–02	10.2	6	–76.1	–24.3
208R-1, 85–87	1778.85	5.31E–01	2.32E–03	8.7	7	–81.5	–8.4
208R-2, 10–12	1779.60	4.62E+00	2.95E–02	6.0	ND	–80.5	ND
208R-2, 99–101	1780.49	5.31E+00	1.64E–02	12.3	7	–81.9	–33.2
209R-1, 29–31	1787.79	2.50E+00	2.08E–02	4.6	ND	–73.9	–19.8
209R-1, 103–105	1788.53	3.20E–02	6.66E–04	1.8	8	–22.5	–4.4
209R-2, 3–5	1789.03	2.70E–02	6.91E–04	1.5	ND	–47.9	ND
209R-2, 9–11	1789.09	9.70E–02	6.79E–04	5.4	4.5	–36.3	–13.9
210R-1, 18–20	1795.08	6.13E+00	2.31E–02	10.1	7.5	–77	ND
210R-1, 27–29	1795.17	5.63E+00	2.83E–02	7.6	ND	–73.8	ND
210R-2, 2–4	1796.42	5.44E+00	3.05E–02	6.8	ND	–74.9	ND
211R-1, 129–131	1799.79	7.48E+00	2.69E–02	10.6	5.5	–71.6	4
213R-1, 49–51	1812.99	4.35E+00	1.47E–02	11.3	6	–82	–13.6
214R-1, 31–33	1818.91	4.70E–02	8.04E–04	2.2	32	–56.8	2.7
214R-1, 44–46	1819.04	1.04E–01	9.82E–04	4.0	ND	–30.2	ND
214R-1, 132–134	1819.92	6.86E+00	3.31E–02	7.9	6	–79.1	–9.7
214R-2, 88–90	1820.98	9.40E–02	3.77E–04	9.5	9.5	–11.4	–13
214R-2, 130–132	1821.40	6.82E+00	3.10E–02	8.4	6	–70	–5.5
217R-1, 4–6	1837.44	4.50E–02	7.92E–04	2.2	20	–56	–2.6
221R-1, 44–46	1875.44	3.26E+00	1.25E–02	9.9	8	–80.6	–12.8
222R-1, 17–19	1884.77	6.12E–01	3.59E–03	6.5	26	–52	–10.9
222R-1, 37–39	1884.97	7.18E–01	4.64E–03	5.9	17	–46.7	–11.7
225R-1, 137–139	1913.57	6.07E+00	2.78E–02	8.3	5.5	–79.1	–15.2
225R-2, 42–44	1914.12	5.04E+00	1.97E–02	9.7	5	–75.7	–18
226R-1, 61–63	1920.61	1.95E+00	8.24E–03	9.0	5	–81.2	–16.3
226R-1, 144–146	1921.44	2.90E–01	2.57E–03	4.3	ND	–75.9	–9.4
226R-2, 66–68	1922.16	2.90E–02	6.07E–04	1.8	ND	–65.6	–0.2
226R-2, 72–74	1922.22	5.61E+00	3.40E–02	6.3	5	–68.2	–12.6
226R-2, 120–122	1922.70	4.75E+00	3.56E–02	5.1	ND	–88.3	ND
226R-3, 2–4	1923.02	5.81E+00	3.16E–02	7.0	5.5	–70.8	–13.9
227R-1, 83–85	1925.33	5.91E+00	3.15E–02	7.2	5.5	–80.7	–19.9
227R-2, 10–12	1926.10	5.30E–02	7.67E–04	2.6	26	–40.7	–17.5
228R-1, 55–57	1934.55	3.54E+00	2.20E–02	6.1	7	–71.5	–10.1
236R-1, 53–55	1981.23	2.37E+00	2.10E–02	4.3	ND	–76.5	–5.5

Note: ND = not determined.

this depth may result from a small remaining component of DIRM. Although significant DIRM components were removed at low demagnetizing fields, it is possible that a small portion of the secondary magnetization was relatively resistant to AF demagnetization. Because the DIRM was steep and negative, a small remaining component would have the effect of slightly steepening the total remaining remanent magnetization of sample below 1560 mbsf. Another explanation for the change in mean I_{stable} value at 1560 mbsf is that the origin (and potentially the direction) of the stable remanent magnetization changes at approximately 1560 mbsf. As will be discussed in later sections, both the dominant style of alteration of magnetite and rock magnetic properties gradually change with depth in the 504B dike section. These results suggest that the upper part of the section may carry a chemical remanent magnetization and the bottom part of the section may carry a viscous or thermal remanent magnetization. However, the alteration of magnetite is observed to change very gradually with depth, whereas the change in mean I_{stable} values is observed to occur abruptly at 1560 mbsf. This is a difficult issue to resolve. One potential solution is to use a different demagnetizing technique (e.g., thermal demagnetization) on additional samples from the bottom part of the dike section. Comparison of I_{stable} values determined using the two demagnetization techniques could confirm whether AF techniques are sufficient to completely remove DIRM.

Rock Magnetic Properties

Hysteresis loop parameters were measured on a subset of the Leg 137/140 dike samples to examine the intrinsic magnetic properties of these rocks and the variation in effective magnetic grain size within the dike section. Saturation magnetization (J_s) measures the total quantity of magnetic material in the sample (minus the paramagnetic component) and is plotted vs. depth in Figure 5. J_s is typically dependent on both the concentration and composition of the magnetic material within a sample. As will be discussed later, the dominant magnetic material in the 504B samples is low-titanium magnetite. In this case, the J_s values can be directly related to the total quantity of magnetite within the individual samples. Figure 5 shows that the amount of magnetite remains relatively constant throughout the entire dike complex with a mean value of 1.07 Am^2/kg. There are, however, a significant number of samples that have J_s values much lower than the mean ($\leq$0.1 Am^2/kg). The samples with low J_s values correspond directly to those samples with low J_0 and k values, implying that a decrease in the total amount of magnetite is responsible for the low magnetization and magnetic susceptibility values.

The ratio of saturation magnetization to saturation remanence (J_{rs}/J_s) is a quantitative way to examine the proportion of magnetic minerals capable of carrying a stable remanent magnetization. This ratio is commonly used to estimate the effective magnetic grain size (e.g., Day et al., 1977) with J_{rs}/J_s values <0.1 indicating the carrier of remanent magnetization is multi-domain, and J_{rs}/J_s values >0.5 indicating the carrier of remanent magnetization is dominated by single-domain grains (Dunlop, 1973). Figure 5 shows values of J_{rs}/J_s for the 504B samples plotted vs. depth. This plot clearly shows that J_{rs}/J_s decreases with depth by a factor of three, and it is interpreted that the effective magnetic grain size of the 504B dike samples increases with depth in the section. The mean J_{rs}/J_s value is 0.19 and indicates that the majority of the 504B dike samples exhibit pseudo-single domain behavior. This indicates that although the average magnetic grain size is larger than that observed for single domain magnetite, the sheeted dike samples are capable of carrying significant stable remanent magnetization. The mean J_{rs}/J_s value for the 504B dikes is very close to that observed for the 504B extrusive basalts (0.23); this indicates the average, effective magnetic grain size of the extrusive basalts and the sheeted dikes is similar.

Bulk coercivity (H_c) measures the strength of the field that is required to drive the saturation magnetization of the sample to zero when measured in an applied field. It is generally used to determine the stability, or hardness, of the remanent magnetization carried by the sample. Values of H_c are plotted vs. depth in Figure 5 and show that there is a factor of 3 decrease in bulk coercivity of the sheeted dikes with depth in the section. This result, which implies the stability of magnetization decreases with depth in the section, is consistent with the interpretation that the effective magnetic grain size increases with depth. As discussed in the following section, optical mineralogy results indicate that a change in the physical size of magnetite is due to a change in the style of alteration with depth.

Table 2. Summary of rock magnetic measurements for Leg 137/140 dike samples.

Core, section, interval (cm)	Depth (mbsf)	J_s (Am^2/kg)	J_{rs}/J_s	H_c (mT)	H_{cr}/H_c	Curie temperature (°)
137-504B-						
173R-2, 20–22	1571.70	1.01	0.219	17.3	1.76	570
180M-2, 49–51	1620.39	1.17	0.171	12.9	1.83	ND
180M-2, 96–98	1620.86	ND	0.209	13.8	1.6	ND
140-504B-						
186R-1, 121–123	1627.51	0.78	0.112	7.9	2.22	530
187R-1, 24–26	1632.24	0.09	0.178	13.1	2.68	ND
189R-1, 96–98	1651.96	ND	0.08	5.35	2.49	ND
189R-1, 101–103	1652.01	0.82	0.075	5.4	3.01	ND
191R-1, 23–25	1661.63	ND	0.088	5.32	2.54	ND
192R-1, 0–2	1670.90	0.89	0.093	6.3	2.33	560
193R-1, 48–50	1674.98	ND	0.291	27.7	1.83	ND
194R-1, 93–95	1681.33	0.78	0.056	4.7	3.87	ND
197R-1, 32–34	1703.12	1.44	0.072	5.8	3.14	ND
200R-1, 109–111	1729.69	0.68	0.156	11	1.92	530
200R-2, 140–142	1731.50	ND	0.147	9.72	1.79	ND
202R-1, 56–58	1747.76	ND	0.161	8.69	1.89	ND
204R-1, 8–10	1756.58	ND	0.086	9.08	3.19	ND
204R-1, 39–41	1756.89	0.15	0.132	12.8	2.54	ND
206R-1, 19–21	1760.89	ND	0.208	15.6	2.47	ND
208R-2, 10–12	1779.60	0.17	0.181	11.2	1.83	ND
208R-2, 103–105	1780.48	ND	0.147	9.17	1.85	ND
208R-2, 108–110	1780.53	0.04	0.176	10.1	1.96	ND
209R-2, 9–11	1789.02	ND	0.165	9.13	1.77	ND
209R-2, 3–5	1789.03	0.01	0.133	11.3	5.18	ND
210R-1, 27–29	1795.17	0.89	0.113	9.6	2.17	ND
211R-1, 96–98	1799.46	0.92	0.112	7.8	2.27	ND
214R-1, 44–46	1819.04	0.03	0.177	16	2.4	ND
214R-2, 111–113	1821.16	0.77	0.124	7.3	2.03	572
214R-2, 130–132	1821.35	ND	0.156	17.8	2.29	ND
218R-1, 24–26	1847.14	0.68	0.082	6.6	2.97	535
220R-1, 2–4	1865.52	0.29	0.091	8.6	3.15	ND
221R-1, 44–46	1875.44	ND	0.147	9.41	1.96	ND
222R-1, 37–39	1884.97	0.13	0.151	14.8	2.42	ND
222R-1, 37–39	1884.97	ND	0.173	14.1	2.34	ND
225R-1, 78–80	1912.98	0.18	0.145	11.1	2.38	ND
226R-1, 144–146	1921.44	0.15	0.137	11.1	3.23	ND
226R-2, 120–122	1922.70	1.72	0.098	7.5	2.29	576
227R-1, 97–99	1925.47	ND	0.116	7.71	2.09	ND
233R-1, 19–21	1960.19	0.72	0.073	5.6	2.88	565
236R-1, 19–21	1980.89	ND	0.234	21.5	2.02	ND
236R-1, 53–55	1981.23	0.87	0.085	5.8	2.7	560

Note: ND = not determined.

Table 3. Mean values of paleomagnetic and rock magnetic parameters for the new Leg 137/140 samples from Hole 504B.

	Mean	Standard deviation	Number of samples
J_0 (A/m)	1.7	1.0	66
k (SI units)	0.016	0.011	66
Q	6.1	2.9	66
MDF (mT)	9.6	6.6	48
I_{stable}	–13	18	47
J_s (Am^2kg^{-1})	0.86	0.66	34
J_{rs}/J_s	0.14	0.05	40
H_c (mT)	10.6	4.8	40
H_{cr}/H_c	2.4	0.68	40
Curie temperature (°C)	555	19	8

Table 4. Mean values of paleomagnetic and rock magnetic parameters for samples from the entire dike complex at Hole 504B.

	Mean	Standard deviation	Number of samples
J_0 (A/m)	2.1	1.7	173
k (SI units)	0.017	0.011	166
Q	5.1	4.0	163
MDF (mT)	17.2	10.9	146
I_{stable}	–5	21	151
J_s (Am^2kg^{-1})	1.07	0.67	94
J_{rs}/J_s	0.19	0.08	76
H_c (mT)	13.8	6.5	67
H_{cr}/H_c	2.3	0.7	58
Curie temperature (°C)	573	20	29

Magnetic Mineralogy

Thermomagnetic measurements were performed on Leg 137/140 samples to constrain the average composition of the magnetic minerals contained in these rocks. The Curie temperature (T_{curie}) values determined for the entire sheeted dike complex, including the Leg 137/140 samples, are plotted vs. depth in Figure 6. The mean T_{curie} value for the entire dike complex sampled at Hole 504B is 573°C (note there is approximately 10° of error in the method). For the Leg 137/140 samples, the mean T_{curie} value is slightly lower, 555°C. The T_{curie} data demonstrate that the dominant magnetic mineral within the dike complex is titanium-poor magnetite (T_{curie} = 582°C for pure magnetite). No low T_{curie} values indicating the presence of high-titanium magnetite were observed.

The initial composition of primary oxide minerals in tholeiitic basalts is well understood (Buddington and Lindsley, 1964; Carmichael and Nicholls, 1967; Petersen, 1979), and previous work has shown that the primary magnetic mineral in tholeiitic basalts from the seafloor is titanomagnetite having an ulvospinel composition near 60% (Bleil and Petersen, 1977; Johnson and Hall, 1978). Because of the presence of geochemically unstable ferrous ions, the oxide minerals contained in igneous rocks generally experience some form of subsolidus alteration. Previous work has shown that the types of alteration most commonly observed to affect titanomagnetite grains are (1) high-temperature deuteric oxidation (>500°–600°C), (2) hydrothermal alteration (200°–400°C), and low-temperature oxidation (<100°C). All of these types of alteration modify the initial composition of titanomagnetite and result in very distinctive changes in the morphology of

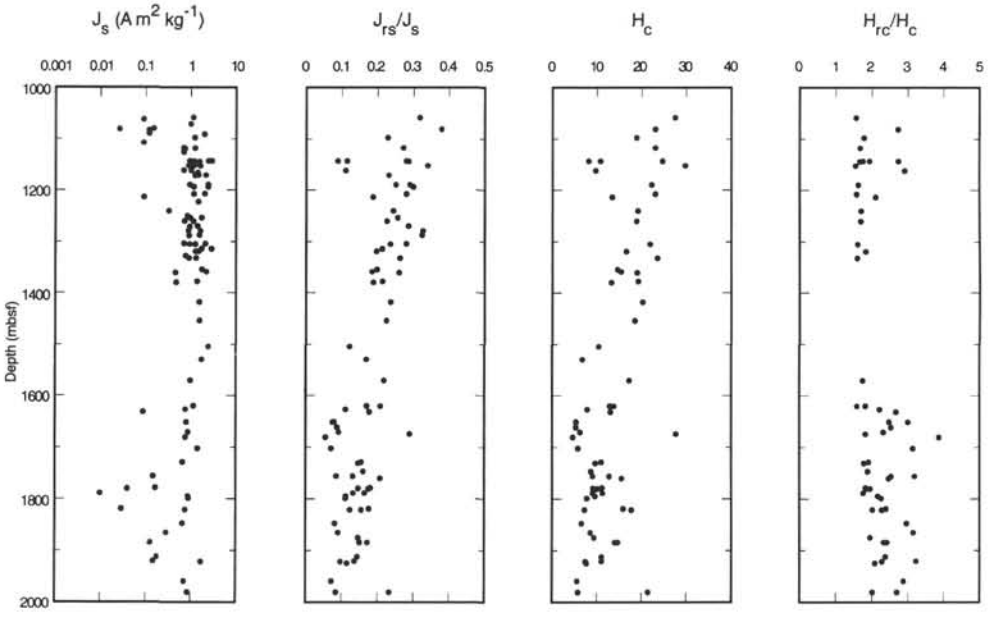

Figure 5. Saturation magnetization (J_s), the ratio of saturation magnetization to saturation remanence (J_{rs}/J_s), bulk coercivity (H_c), and the ratio of coercivity or remanence and bulk coercivity (H_{rc}/H_c) plotted vs. depth for 504B dike samples. Note that J_s is plotted on a log scale.

the original titanomagnetite (see Figs. 7 and 8; also Ozima and Larson, 1970; Ade-Hall et al., 1971; Haggerty, 1976; Hall and Fisher, 1987). By studying the oxide petrography of igneous rocks, it is often possible to constrain their thermal and alteration history. In this paper, we use oxide petrography to understand the post-emplacement crustal formation processes that have modified the sheeted dike complex and the effect of these changes on the magnetic properties of the dike rocks.

Oxide minerals were examined both in air and in oil at magnifications from 28× to 1200× using a Zeiss photomicroscope and were observed to have undergone two subsolidus processes: high-temperature deuteric oxidation and hydrothermal alteration. We use the classification scheme of Ade-Hall et al. (1968) to describe the degree of deuteric oxidation experienced by primary titanomagnetite grains. In this system, C1 titanomagnetites are optically uniform grains with no exsolution features, C2 titanomagnetite grains have a small number of ilmenite lamellae oriented parallel to the (111) octahedral planes of the host, and C3 titanomagnetite grains consist of 50% or more ilmenite lamellae. Higher grades of deuteric alteration were not observed. To describe the hydrothermal alteration of titanomagnetite, we used a classification scheme based on Hall and Fisher (1987). In this system, H1 titanomagnetites have not been visibly altered by a hydrothermal fluid, H2 grains are characterized by the presence of fine anatase/rutile granules within the host titanomagnetite or by the incipient replacement of ilmenite lamellae by sphene, H3 grains are completely granulated to anatase/rutile and magnetite or show complete replacement of ilmenite lamellae by sphene, H4 titanomagnetite grains are similar to H3 grains but have areas of iron loss in the magnetite host, H5 grains have lost at least 50% of the iron in the host magnetite and show complete replacement of ilmenite lamellae by sphene, and H6 grains have no magnetite remaining and consist completely of anatase or rutile.

Twenty-eight thin sections recovered during Legs 137/140 were examined and all were observed to have abundant primary magnetite (~1%), which was generally interstitial to plagioclase and pyroxene. The initial grain size of the titanomagnetite was variable but was most commonly from 50 to 150 mm and was similar in size to the primary silicate minerals. High-temperature oxidation of primary titanomagnetite to magnetite and ilmenite was observed in most samples. In these samples, ilmenite lamellae were very well-developed (generally C3 type grains; see Plate 1A) and clearly visible at relatively low magnifications (200×). However, for samples that experienced high degrees of hydrothermal alteration, it was sometimes difficult to assess the initial degree of high-temperature deuteric oxidation. In addition, two very fine-grained samples did not show evidence of deuteric oxidation. The primary titanomagnetite grains observed in these two samples were skeletal in form and had experienced no significant subsolidus alteration. This observation suggests that these two samples cooled very soon after emplacement. The two fine-grained samples likely were from very narrow dikes, or near dike margins. Another possibility is that these two samples were actually drilling rubble knocked into the bottom of the hole from the upper, extrusive portion of the drilled section.

The pervasive, high-temperature oxidation of titanomagnetite observed in the Leg 137/140 samples is in contrast to the upper part of the sheeted dike complex (Pariso and Johnson, 1991). In the upper 300 m of the dike complex, evidence for oxidation of titanomagnetite to ilmenite and magnetite is rarely observed. At 1358 mbsf (about 300 m into the dike complex), very fine and discontinuous ilmenite lamellae in primary titanomagnetite are first observed as a common feature of the diabase. With depth in the section, the presence of ilmenite within a magnetite host becomes more common, but well-developed ilmenite lamellae are not typical. Rather, the morphology of the ilmenite "exsolution" bodies in this part of the dike complex are as discontinuous lamellae, or as irregular, pod-like forms. Although these irregular ilmenite shapes are clearly present in some Leg 137/140 samples, the most common morphology displayed by the secondary ilmenite is well-developed lamellae. These observations suggest that there was a significant decrease in the rate of cooling of the sheeted dike complex with depth.

Hydrothermal alteration of titanomagnetite is common in all samples examined, but the degree of alteration varies substantially between samples (see Plates 1A, -B, and -C). Most of the samples examined show evidence of light to moderate degrees of hydrothermal alteration (H2 and H3 type grains) with ilmenite lamellae partially to completely replaced by sphene. The degree of hydrothermal alteration of ilmenite and titanomagnetite appears to be well-correlated with the degree of alteration of silicate minerals. In addition, pyroxene grains that are altered to chlorite and actinolite are nearly always adjacent to hydrothermally altered titanomagnetite, suggesting chemical exchange between the primary titanomagnetite and the secondary silicate minerals (see Plate 1D). For a small but significant number of samples, the degree of hydrothermal alteration of titanomagnetite is very high (H5 and H6 type grains), and the ilmenite/magnetite net-

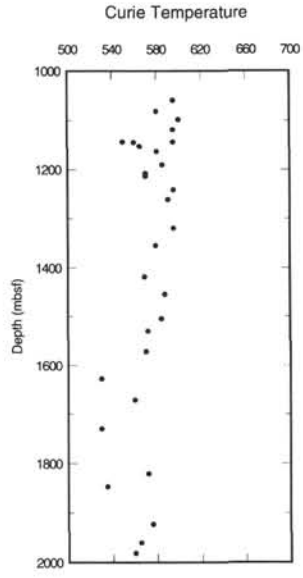

Figure 6. Values of Curie temperature plotted vs. depth for 504B dike samples.

works are partially to completely replaced by sphene and anatase or rutile (Plate 1C). As a result, these highly altered grains are no longer completely opaque, and, in fact, are easily examined in transmitted light. The samples that experienced high degrees of hydrothermal alteration, and corresponding high degrees of iron loss in the ilmenite/magnetite networks, correspond to samples that were observed to have low J_0, k, and J_s values. These results demonstrate that the very low values of these parameters are a direct result of variable degrees of hydrothermal alteration. Overall, about 10%–15% of the rocks recovered during Legs 137/140 have experienced very high degrees of hydrothermal alteration (i.e., 60%–80% replacement of primary silicate minerals; see Alt, Zuleger, Erzinger, this volume).

Secondary magnetite, observed as fine-grained along the cleavage planes of pyroxene, is common. Similarly, when relict olivine is present it is commonly altered to the assemblage talc/chlorite/magnetite.

DISCUSSION

Crustal Formation Processes

The degree of high-temperature (deuteric) alteration experienced by primary titanomagnetite grains clearly increases with depth in the dike samples from Hole 504B. Because virtually no high-temperature oxidation of titanomagnetite is observed in the upper dike rocks, we can infer that this part of the crustal section cooled relatively quickly. In contrast, the lower dike rocks sampled during Legs 111, 137, and 140 show increasing degrees of high-temperature oxidation, and this implies they cooled at a slower rate. The decrease in initial cooling rate with depth is likely to be a result of decreasing crustal permeability. The porosity of the 504B dike samples is very low (see Iturrino et al., this volume) and shows a decrease with depth (from 2% to 0.5%). However, it is unclear whether the permeability changes are related to primary porosity (i.e., initial grain/grain boundary porosity) or secondary porosity (i.e., fracture porosity). Most of the primary titanomagnetite grains have experienced light to moderate degrees of hydrothermal alteration. There appears to be a decrease with depth in the abundance of secondary minerals (sphene, anatase, or rutile) formed from the interaction of titanomagnetite and ilmenite with hydrothermal fluid. Because low-titanium magnetite is chemically more stable than titanomagnetite, this is due, at least in part, to the increase in high-temperature oxidation of titanomagnetite with depth (see Fig. 7). However, if initial permeability did decrease as a function of depth, the decrease in hydrothermal alteration of titanomagnetite and ilmenite with depth could also be a result of lower water/rock ratios.

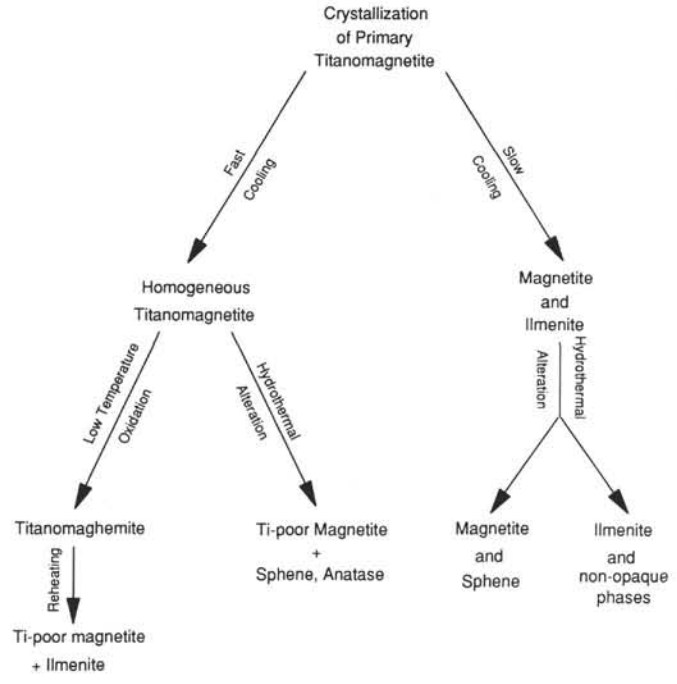

Figure 7. Simplified summary of possible cooling and alteration histories of a primary titanomagnetite grain (after Pariso and Johnson, 1991).

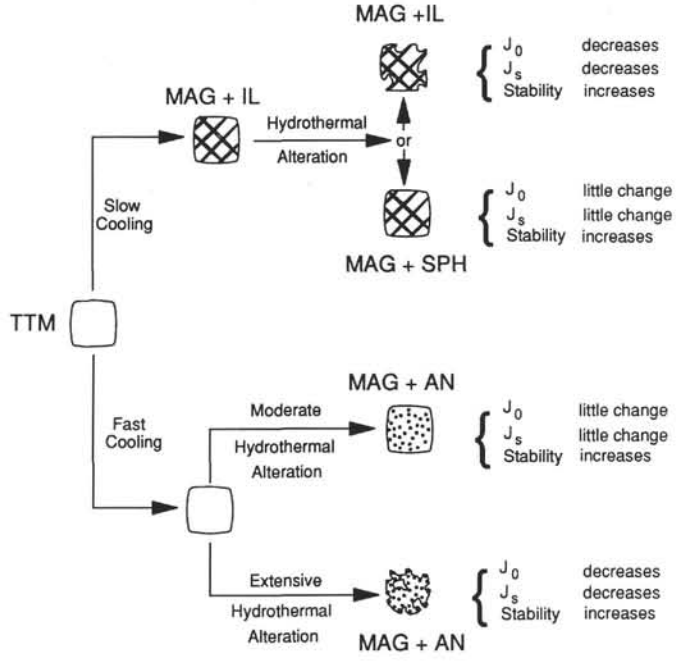

Figure 8. The possible cooling and alteration histories of a primary titanomagnetite grain, and the resulting opaque mineral phases and textures. TTM = titanomagnetite; MAG = magnetite; IL = ilmenite; AN = anatase; SPH = sphene. This diagram is based on previous observations of these alteration assemblages: (1) Buddington and Lindsley (1964), (2) Ade-Hall et al., (1968), (3) Haggerty (1976), (4) Ade-Hall et al., (1971), and (5) Hall and Fisher (1987) (after Pariso and Johnson, 1991).

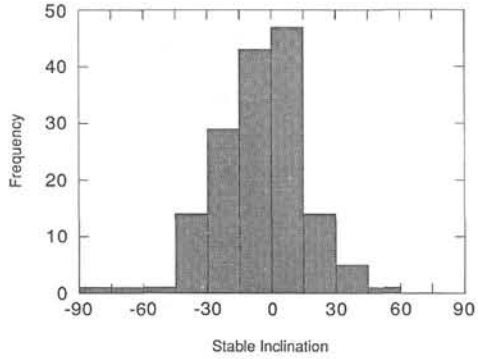

Figure 9. Histogram of stable inclination values for 504B dike samples.

A small percentage of the recovered core (10%) experienced very high degrees of hydrothermal alteration (60%–80% alteration of silicate minerals). In these samples, primary titanomagnetite grains were heavily altered also. Although the highly altered samples represent 10% of the recovered core, it is difficult to extend these results to the entire drilled section because the average recovery of core was only 12%. Therefore, there appears to be some uncertainty regarding the "true" percentage of heavily altered samples.

Implications for Magnetic Anomalies

Although titanomagnetite was the initial (igneous) magnetic phase within the dike samples, the carrier of magnetization throughout the dike section is low-titanium magnetite. In the upper part of the dike section, the low-titanium magnetite is produced by hydrothermal alteration of titanomagnetite. In the lower part of the section, low-titanium magnetite is produced by high-temperature deuteric oxidation. This suggests that there may be a difference in the origin of remanent magnetization throughout the dike section, with the upper dikes carrying a chemical remanent magnetization (CRM) and the lower dikes carrying a thermal remanent magnetization (TRM). However, despite the possible difference in the origin of the remanent magnetization, there is only a small change in the stable magnetic inclination within the dike section (Figs. 5 and 9). Thus there is not strong direct evidence for two different magnetization events.

The remanent and rock magnetic parameters observed in the 504B dike samples are influenced by post-emplacement alteration, and the change in the dominant style of alteration with depth correlates with decreasing stability of remanent magnetization. Overall, the remanent and rock magnetic data suggest that the sheeted dike rocks are capable of contributing to marine magnetic anomalies. The intensity of remanent magnetization (J_0) has an average value of 2.1 A/m, about half the value observed in the overlying extrusives (5.6 A/m). As the dike section cored so far is about twice as thick as the extrusives, it could produce a magnetic anomaly of similar amplitude (see Pariso and Johnson, 1991, for a direct calculation of the expected anomaly). Similarly, the Q values of the dike samples are all greater than 1. This implies that the in-situ magnetization is dominated by remanent, rather than induced, magnetization. Finally, J_{rs}/J_s ratios observed in the dike samples are similar to those observed in the 504B extrusive basalts and suggest that both the basalts and dikes are capable of carrying significant stable remanent magnetization. However, there are several outstanding questions regarding the ability of the sheeted dikes to contribute to marine magnetic anomalies.

First, the equilibrium bottom-hole temperature within 504B is about 200°C, and this might have the effect of reducing the relaxation time of the remanent magnetization. Thus it is possible that these samples have a significant component of viscous remanent magnetization (VRM). Although room temperature VRM experiments showed no significant change in NRM, experiments conducted at higher temperatures are necessary to reproduce the current geological conditions at 504B. Second, although MDF and H_c values suggest that the dike samples, on average, have a moderate magnetic stability, the stability does decrease with depth. The high in-situ temperature might further reduce the stability of remanent magnetization so that the relaxation time is, on a geological time scale, quite short. In this case, the observed remanent magnetization might actually be a VRM acquired in the ambient magnetic field. Because the 504B crustal section was formed during a period of reversed geomagnetic polarity, this scenario suggests the potential for two different directions of magnetization: (1) a TRM or CRM pointing south in the original direction, and (2) a VRM pointing north in the direction of the ambient field. Unfortunately, the direction of remanent magnetization is in the horizontal plane, and it is not possible to determine its polarity with the unoriented cores recovered from Hole 504B.

Finally, compared with many ophiolites (e.g., Troodos, Samail, and the Josephine; see Lippard et al., 1986; Harper et al., 1988; Baragar et al., 1990; Gillis and Robinson, 1990; Nehlig and Juteau, 1988), alteration in the 504B dike complex is surprisingly low, averaging only 10%–20% with a small percentage of rocks having much higher degrees of alteration (Alt et al., 1986; Alt, Zuleger, Erzinger, this volume). Although this result initially suggests an important difference in the nature of fluid flux between ophiolites and the crust at Hole 504B, it must be viewed with caution because only 13% of the dike section has been recovered. The 504B crustal section is heavily sedimented, and it was probably sealed to active hydrothermal alteration at a relatively young age. It is thus possible that the crustal section at Site 504 has experienced less hydrothermal alteration than "typical" oceanic crust. Because the degree of hydrothermal alteration clearly has a strong effect on the remanent magnetization of the 504B dike rocks, this remains an important question regarding the ability of lower crustal rocks to contribute to marine magnetic anomalies. Further sampling of in-situ oceanic crust is likely to be the only means of addressing this problem directly.

SUMMARY

Oxide petrography results show a strong gradient in the type of alteration experienced by primary titanomagnetite in dike rocks recovered from Hole 504B. In the upper part of the dike complex, hydrothermal alteration is dominant and high-temperature oxidation is rare. In the lower portion of the dike complex, high-temperature oxidation of titanomagnetite to ilmenite and magnetite is pervasive and is followed by moderate amounts of hydrothermal alteration. Both types of alteration result in the formation of low-titanium magnetite—the dominant magnetic phase in the dike complex. These alteration events reduce the magnetic grain size of the primary titanomagnetite grains and result in a remanent magnetization that is moderately stable. A gradual decrease in the magnetic stability of the dike samples with depth corresponds to the variation in the type of alteration of magnetite with depth and suggests that hydrothermal alteration (which dominates alteration of primary titanomagnetite in the upper dike complex) is somewhat more effective at reducing the magnetic grain size. Paleomagnetic and rock magnetic measurements on dike samples from Hole 504B indicate that, on average, the dikes are capable of carrying a moderately strong, stable remanent magnetization. The magnetic properties of the dikes are similar to those of the overlying extrusive basalts. These results suggest that the sheeted dike complex sampled at Hole 504B may contribute to an overlying marine magnetic anomaly.

ACKNOWLEDGMENTS

This work was supported by the JOI/USSAC fund for post-cruise science. We wish to thank Paul Johnson and Lisa Tauxe for the use of their labs at the University of Washington and Scripps Institute of Oceanography, respectively. We also wish to thank the Institute for Rock Magnetism at the University of Minnesota. The IRM is funded

by the Keck Foundation, the National Science Foundation, and the University of Minnesota. Finally, constructive reviews by Jim Hall, Guy Smith, and Keir Becker helped improve this manuscript.

REFERENCES*

Ade-Hall, J.M., and Johnson, H.P., 1976. Paleomagnetism of basalts, Leg 34. *In* Yeats, R.S., Hart, S.R., et al., *Init. Repts. DSDP,* 34: Washington (U.S. Govt. Printing Office), 513–532.

Ade-Hall, J.M., Khan, M.A., Dagley, P., and Wilson, R.L., 1968. A detailed opaque petrological and magnetic investigation of a single tertiary lava flow from Skye, Scotland. I: Iron-titanium oxide petrology. *Geophys. J. R. Astron. Soc.,* 16:375–388.

Ade-Hall, J.M., Palmer, H.C., and Hubbard, T.P., 1971. The magnetic and opaque petrological response of basalts to regional hydrothermal alteration. *Geophys. J. R. Astron. Soc.,* 24:137–174.

Alt, J.C., Anderson, T.F., Bonnell, L., and Muehlenbachs, K., 1989. Mineralogy, chemistry, and stable isotopic compositions of hydrothermally altered sheeted dikes: ODP Hole 504B, Leg 111. *In* Becker, K., Sakai, H., et al., *Proc. ODP, Sci. Results,* 111: College Station, TX (Ocean Drilling Program), 27–40.

Alt, J.C., Honnorez, J., Laverne, C., and Emmermann, R., 1986. Hydrothermal alteration of a 1 km section through the upper oceanic crust, Deep Sea Drilling Project Hole 504B: mineralogy, chemistry, and evolution of seawater-basalt interactions. *J. Geophys. Res.,* 91:10309–10335.

Anderson, R.N., and Hobart, M.A., 1976. The relation between heat flow, sediment thickness, and age in the Eastern Pacific. *J. Geophys. Res.,* 81:2968–2989.

Baragar, W.R.A., Lambert, M.B., Baglow, N., and Gibson, I.L, 1990. The sheeted dyke zone in the Troodos Ophiolite. *In* Malpas, J., Moores, E.M., Panayiotou, A., Xenophontos, C. (Eds.), *Ophiolites: Oceanic Crustal Analogues,* Nicosia, Cyprus (Geological Survey Department), 37–51.

Becker, K., Foss, G., et al., 1992. *Proc. ODP, Init. Repts.,* 137: College Station, TX (Ocean Drilling Program).

Becker, K., Sakai, H., Adamson, A.C., Alexandrovich, J., Alt, J.C., Anderson, R.N., Bideau, D., Gable, R., Herzig, P.M., Houghton, S.D., Ishizuka, H., Kawahata, H., Kinoshita, H., Langseth, M.G., Lovell, M.A., Malpas, J., Masuda, H., Merrill, R.B., Morin, R.H., Mottl, M.J., Pariso, J.E., Pezard, P.A., Phillips, J.D., Sparks, J.W., and Uhlig, S., 1989. Drilling deep into young oceanic crust, Hole 504B, Costa Rica Rift. *Rev. Geophys.,* 27:79–102.

Bleil, U., and Petersen, N., 1977. Magnetic properties of basement rocks, Leg 37, Site 332. *In* Aumento, F., Melson, W.G., et al., *Init. Repts. DSDP,* 37: Washington (U.S. Govt. Printing Office), 449–456.

Buddington, A.F., and Lindsley, D.H., 1964. Iron-titanium oxides minerals and synthetic equivalents. *J. Petrol.,* 5:310–357.

Carmichael, I.S.E., and Nicholls, J., 1967. Iron-titanium oxides and oxygen fugacities in volcanic rocks. *J. Geophys. Res.,* 72:4665–4687.

Day, R., Fuller, M., and Schmidt, V.A., 1977. Hysteresis properties of titanomagnetites: grain-size and compositional dependence. *Phys. Earth Planet. Inter.,* 13:260–267.

Dick, H.J.B., Erzinger, J., Stokking, L.B., et al., 1992. *Proc. ODP, Init. Repts.,* 140: College Station, TX (Ocean Drilling Program).

Dunlop, D.J., 1973. Superparamagnetic and single-domain threshold sizes in magnetite. *J. Geophys. Res.,* 78:1780–1793.

Gillis, K.M., and Robinson, P.T., 1990. Patterns and processes of alteration in the lavas and dykes of the Troodos Ophiolite, Cyprus. *J. Geophys. Res.,* 95:21523–21548.

Haggerty, S.E., 1976. Oxidation of opaque mineral oxides in basalts. *In* Rumble, D., III (Ed.), *Oxide Minerals.* Mineral. Soc. Am. Short Course Notes, 3:101–140.

Hall, J.M., and Fisher, B.E., 1987. The characteristics and significance of secondary magnetite in a profile through the dike component of the Troodos, Cyprus, ophiolite. *Can. J. Earth Sci.,* 24:2141–2159.

Harper, G.D., Bowman, J.R., and Kuhns, R., 1988. A field, chemical and stable isotopic study of subseafloor metamorphism of the Josephine Ophiolite, California-Oregon. *J. Geophys. Res.,* 93:4625–4656.

Honnorez, J., Laverne, C., Hubberten, H.-W., Emmermann, R., and Muehlenbachs, K., 1983. Alteration processes in Layer 2 basalts from Deep Sea Drilling Project Hole 504B, Costa Rica Rift. *In* Cann, J.R., Langseth, M.G., Honnorez, J., Von Herzen, R.P., White, S.M., et al., *Init. Repts. DSDP,* 69: Washington (U.S. Govt. Printing Office), 509–546.

Johnson, H.P., and Hall, J.M., 1978. A detailed rock magnetic and opaque mineralogy study of the basalts from the Nazca Plate. *Geophys. J. R. Astron. Soc.,* 52:45–64.

Langseth, M.G., Cann, J.R., Natland, J.H., and Hobart, M., 1983. Geothermal phenomena at the Costa Rica Rift: background and objectives for drilling at Deep Sea Drilling Project Sites 501, 504, and 505. *In* Cann, J.R., Langseth, M.G., Honnorez, J., Von Herzen, R.P., White, S.M., et al., *Init. Repts. DSDP,* 69: Washington (U.S. Govt. Printing Office), 5–29.

Lippard, S.J., Shelton, A.W., and Gass, I.G., 1986. *The Ophiolite of Northern Oman.* Geol. Soc. London Mem., 11.

Lowrie, W., and Kent, D.V., 1978. Characteristics of VRM in ocean basalts. *J. Geophys.,* 44:297–315.

Nehlig, P., and Juteau, T., 1988. Deep crustal seawater penetration and circulation at ocean ridges: evidence from the Oman Ophiolite. *Mar. Geol.,* 84:209–228.

Newmark, R.L., Anderson, R.N., Moos, D., and Zoback, M.D., 1985. Sonic and ultrasonic logging of Hole 504B and its implications for the structure, porosity, and stress regime of the upper 1 km of the oceanic crust. *In* Anderson, R.N., Honnorez, J., Becker, K., et al., *Init. Repts. DSDP,* 83: Washington (U.S. Govt. Printing Office), 479–510.

Ozima, M., and Larson, E.E., 1970. Low- and high-temperature oxidization of titanomagnetite in relation to irreversible changes in the magnetic properties of submarine basalts. *J. Geophys. Res.,* 75:1003–1017.

Pariso, J.E., and Johnson, H.P., 1989. Magnetic properties and oxide petrography of the sheeted dike complex in Hole 504B. *In* Becker, K., Sakai, H., et al., *Proc. ODP, Sci. Results,* 111: College Station, TX (Ocean Drilling Program), 159–167.

———, 1991. Alteration processes at Deep Sea Drilling Project/Ocean Drilling Program Hole 504B at the Costa Rica Rift: implications for magnetization of oceanic crust. *J. Geophys. Res.,* 96:11703–11722.

Pariso, J.E., Scott, J.H., Kikawa, E., and Johnson, H.P, 1991. A magnetic logging study of Hole 735B gabbros at the Southwest Indian Ridge. *In* Von Herzen, R.P., Robinson, P.T., et al., *Proc. ODP, Sci. Results,* 118: College Station, TX (Ocean Drilling Program), 309–321.

Petersen, N., 1979. Rock- and paleomagnetism of basalts from Site 396B, Leg 46. *In* Dmitriev, L., Heirtzler, J., et al., *Init. Repts. DSDP,* 46: Washington (U.S. Govt. Printing Office), 357–362.

Smith, G.M., and Banerjee, S.K., 1986. The magnetic structure of the upper kilometer of the marine crust at Deep Sea Drilling Project Hole 504B, Eastern Pacific Ocean. *J. Geophys. Res.,* 91:10337–10354.

Zijderveld, J.D.A., 1967. AC demagnetization of rocks: analysis of results. *In* Collinson, D.W., Creer, K.M., and Runcorn, S.K. (Eds.), *Methods in Palaeomagnetism:* New York (Elsevier), 254–286.

* Abbreviations for names of organizations and publications in ODP reference lists follow the style given in *Chemical Abstracts Service Source Index* (published by American Chemical Society).

Date of initial receipt: 15 July 1993
Date of acceptance: 5 January 1994
Ms 137/140SR-028

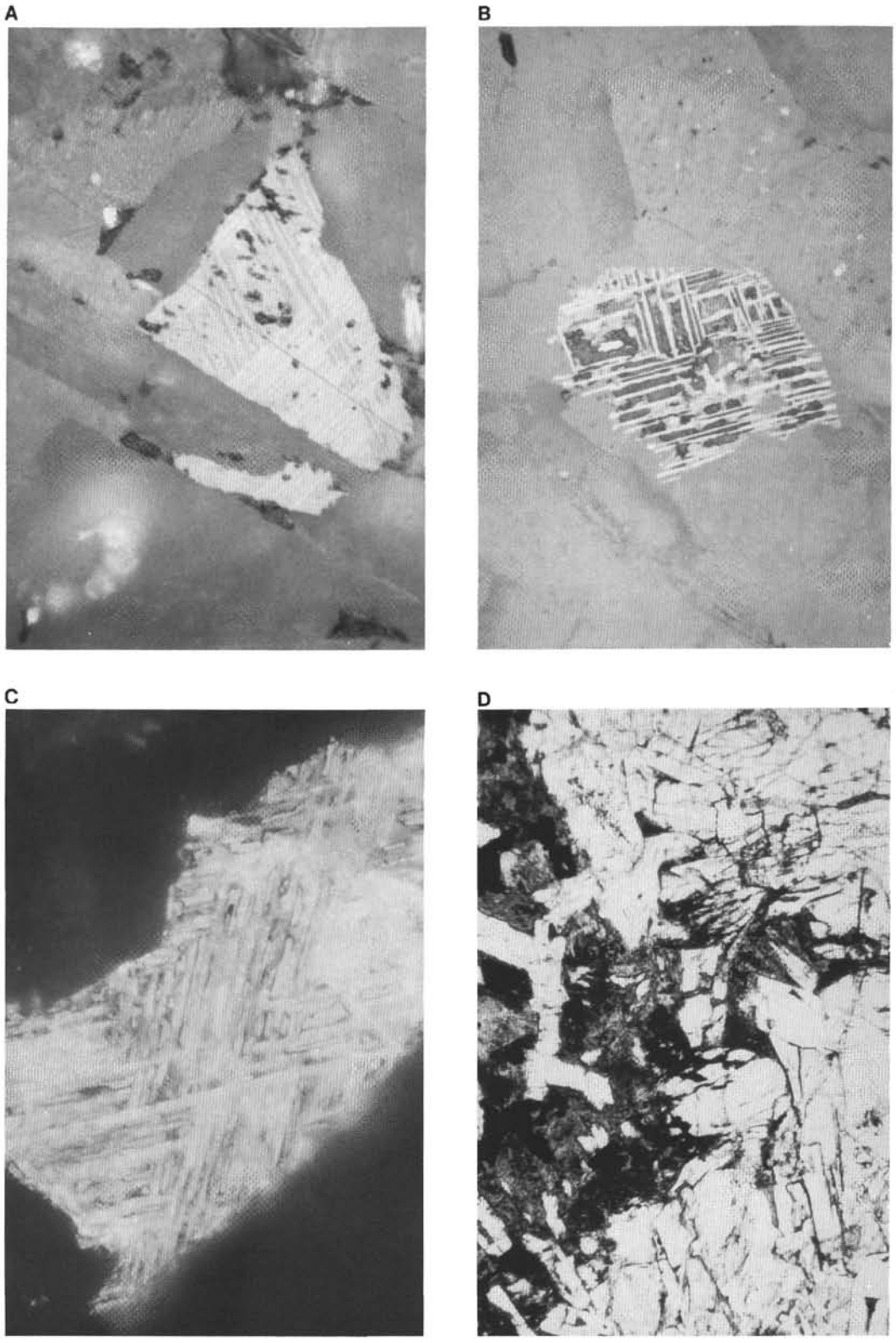

Plate 1. **A.** This photomicrograph shows ilmenite lamellae formed during high- temperature deuteric oxidation within a primary titanomagnetite host. Note that virtually no hydrothermal alteration products are present. **B.** This photomicrograph shows a primary titanomagnetite grain that has experienced high-temperature deuteric alteration to ilmenite/magnetite. The iron in the magnetite was leached during hydrothermal alteration leaving only the ilmenite lamellae. **C.** This photomicrograph shows a primary titanomagnetite grain that has experienced high-temperature deuteric alteration to ilmenite/magnetite. As a result of heavy hydrothermal alteration, the ilmenite lamellae (bright lamellae) were altered to anatase. The iron in the host magnetite has been removed. Note that this grain is nearly transparent to light. **D.** This photomicrograph shows that alteration of pyroxene to chlorite and actinolite commonly occurs adjacent to primary titanomagnetite grains. The long dimension of all photomicrographs is 220 μm.